Electronic Supporting Information (ESI)

Destabilization of DNA through interstrand crosslinking by UO_2^{2+}

André Rossberg, Takaya Abe, Koji Okuwaki, Astrid Barkleit, Kaori Fukuzawa, Tatsuya Nakano, Yuji Mochizuki, Satoru Tsushima

Methodology

Sample preparation. Samples for U–sugar phosphate experiments were prepared as follows. Sugar phosphate disodium salt hydrates (glucose-1-phosphate, G1P, fructose-6-phosphate, F6P and fructose-1,6-diphosphate, F(1,6)P) were purchased from Sigma (analytical grade). The stock solutions (0.1 M) were prepared freshly for each experiment. The stock solution of UO_2^{2+} (0.1 M) was made from $UO_2(NO_3)_2 \cdot 6H_2O$ (Merck, p.A.). The uranyl nitrate was converted in a muffle furnace at 320 °C, the resulting UO_3 was dissolved in 0.5 M $HClO_4$. The concentrations of the EXAFS solutions were adjusted to 1 mM UO_2^{2+} and 50 mM sugar phosphate. The ionic strength was adjusted to 0.1 M by adding $NaClO_4$ ($NaClO_4 \cdot H_2O$, Merck, p.A.) from a 1 M stock solution. All solutions were prepared with deionized water. Necessary pH adjustments were made with $HClO_4$ or NaOH. Samples for U–DNA experiments were prepared as follows. Salmon testes genomic DNA (CALBIOCHEM) was dialyzed against Millipore water resulting in a Na/P ratio of 1.4 and negligible amounts of Ca^{2+} and Mg^{2+} as determined by inductively coupled plasma mass spectrometry using an ICP-MS-ELAN 9000 spectrometer (PerkinElmer SCIEX, Rodgau-Jügesheim, Germany). Uranium concentration was varied from 1 to 5 mM and DNA/U ratio was kept at 4 to 5. The pH of the U-DNA samples was between 5.97 and 6.30. All samples were prepared by mixing following 3 solutions in different ratio; 1) 25 mM DNA stock solution in 5mM acetate buffer, 2) 100 mM U(VI) stock solution, 3) 5 mM acetate buffer. As references a sample of aqueous U(VI) hydrate ($UO_2(H_2O)_5^{2+}$) and the phosphate mineral meta-autunite were prepared. For each sample the chemical conditions are listed in **Table S1**.

Table S1. Samples prepared for EXAFS measurements.[a]

Sample ID	[U] / mM	Ligand	[L] / mM	pH	State
meta-autunite reference					
R1	/	/	/	/	Solid
U(VI) with DNA, fructose-6-phosphate (F6P) and fructose-1,6-diphosphate (F(1,6)P)					
M1	5	DNA	20	6.0	Shock-Frozen
M2	2.5	DNA	10	6.1	Shock-Frozen
M3	2	DNA	10	6.2	Liquid
M4	1	DNA	5	6.3	Liquid
M5	1	F6P	50	4.0	Liquid
M6	1	F6P	50	3.5	Liquid
M7	1	F6P	50	5.5	Liquid
M8	5	F6P	50	5.5	Liquid
M9	/	F(1,6)P	/	/	Solid
M10	1	G1P	50	2.0	Liquid
M11	1	G1P	50	2.5	Liquid
M12	1	G1P	50	3.0	Liquid
M13	1	G1P	50	3.5	Liquid
M14	1	G1P	50	4.0	Liquid
M15	1	G1P	50	4.5	Liquid
M16	1	G1P	50	5.0	Liquid
U(VI) hydrate reference					
R2	20	/	/	1.0	Liquid

[a] The order of the samples here corresponds to the order of the EXAFS spectra in Fig. 1.

EXAFS measurements. The U L_{III}-edge (17185 eV) EXAFS spectra of U containing DNA and sugar phosphate samples were measured at the Rossendorf Beamline (ROBL, BM20) at the European Synchrotron (ESRF).[1] The electron beam (6 GeV, 200 mA) was monochomatized by a water cooled Si(111) double crystal monochromator in channel cut mode (5-35 keV), while higher harmonics where rejected with two Rh-coated mirrors. Depending on the U-content either the fluorescence signal of the U $L\alpha_{1,2}$ lines or the absorption signal was detected by using a 13-element Ge-detector or gas filled ionization chambers. For each sample multiple energy scans were performed and averaged in order to obtain a sufficient high signal-to-noise ratio and a Y K-edge (17038 eV) absorption spectrum of a Y metal foil was measured simultaneously for energy calibration. The samples were measured at room temperature, except the shock frozen DNA samples which were measured at 15 K in a closed-cycle He-cryostate (**Table S1**). The EXAFS signal was extracted from the raw absorption spectra by using the program suite of EXAFSPAK [2] which contains standard procedures for the statistical weighting of the detectors fluorescence channels and their dead-time correction, energy calibration, removal of the background absorbance and for the shell fitting. The energy scale was converted into the photoelectron wave vector (k), by assuming an ionization potential of E_0 = 17185 eV, while the shift in energy threshold (ΔE_0) was defined as a free parameter with $\Delta E_0 = E_0 - E$t (E_t − theoretical ionization potential) during the shell fit procedure. The maximum available k-range of 3.1 $Å^{-1}$ – 12.1 $Å^{-1}$ leads to a maximum radial resolution of 0.18 Å. For the shell fit theoretical scattering phase and amplitude functions were calculated by the ab-initio scattering code FEFF 8.20 [3] by using the crystal structure of meta-autunite [4] and a structural model for U(VI) hydrate (**Figure S1**). In the case of meta-autunite the EXAFS spectrum was Fourier filtered in the R-range of 0.00 Å - 3.77 Å in order to remove the backscattering signals from higher shells, which are not expected in the systems with DNA and sugar phosphates.

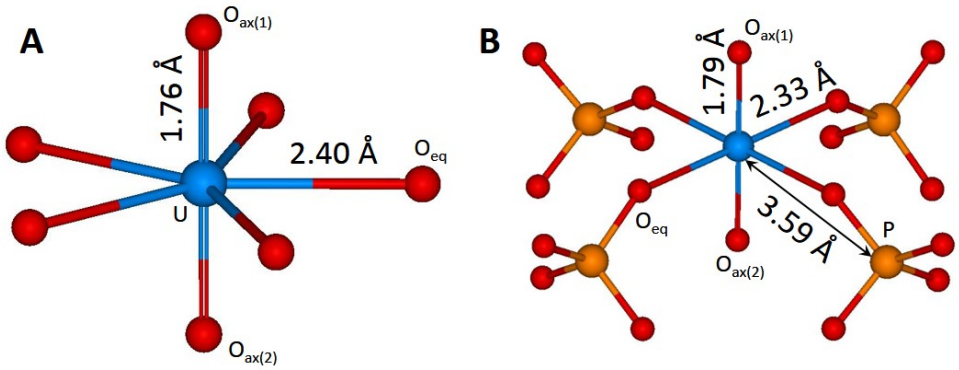

Figure S1. Structural model of U(VI) hydrate (A) and meta-autunite (B) used for FEFF calculation. Radial distances are taken from literature.[4-5] O_{ax} – axial oxygen, O_{eq} – equatorial oxygen. Hydrogen atoms were omitted.

Iterative transformation factor analysis (ITFA).[5-6]

An EXAFS spectrum can be understood as a spectral mixture of the backscattering signals from atoms which surround the X-ray absorbing atom (U) in its local environment, hence as a linear combination of the signals stemming from coordinated atoms or functional groups weighted by their respective coordination number (*CN*). Moreover, if several structurally different metal complexes coexist, then the EXAFS spectrum will be a linear combination of the spectra of the single complexes weighted by their respective fractions. Thus for EXAFS, a linear mixing model, such as the Beer-Lambert law, can be applied. However, the fractions or *CN* might change as a function of a physicochemical parameter (i.e. pH, temperature, concentration, etc.), so that a series of spectral mixtures occurs.

ITFA is a well-established statistical approach aimed at the decomposition of such mixtures into their spectral components and their respective fractions or *CN* for each mixture.[5-16]

ITFA comprises three steps.

1) The *c* spectral mixtures are decomposed by principal component analysis (PCA) [17] into a set of *c* eigenvectors which enable a complete reproduction of the spectral mixtures by their linear combination. However, if the number of spectral components (*n*) is $n<c$ then only *n* eigenvectors are necessary for a sufficient reproduction. The remaining *c*-*n* eigenvectors contain only parts of the experimental error and are rejected, leading to a de-noising of the spectral mixtures by a factor of $(c/n)^{1/2}$. The estimation of *n* is accomplished by the use of the indicator (*IND*) [18] function which reaches a minimum at *n*. With known *n* the root mean square error (*RE*) [18], i.e. the experimental error, is determined.

2) The VARIMAX [19] procedure allows a qualitative measure of the fractions or *CN* of the spectral components by using the *n* eigenvectors calculated by PCA. The application of this step was not necessary for the actually investigated systems.

3) For the final decomposition the iterative target test (ITT) [20] is used. The eigenvectors are transformed via non-orthogonal rotation of the *n*-dimensional factor space into the spectra and the fractions or *CN* of the spectral components by using constrains. In order to receive a unique solution n^2-*n* fractions or *CN* must be fixed at a known value during the iteration. For the

fractions or *CN* the 95% confidence intervals are estimated by using the errors calculated with the method as described by Roscoe et al..[21-22]

EXAFS data analysis and application of ITFA.

The aqueous system of the U(VI):G1P complexes serves as a measure of the applicability of our proposed analysis strategy used for the quantification of coordinated phosphate groups in the system of U(VI) with DNA and other sugar phosphates.

In aqueous solutions and depending on the pH 1:1 and 1:2 U(VI):sugar phosphate complexes are expected in which the sugar phosphate groups interact with U(VI).[23] During complexation and with rising pH coordinated water molecules are exchanged by phosphate groups. In order to determine the number of coordinated water molecules and phosphate groups ITFA is used, while the EXAFS spectra of aqueous U(VI) hydrate and meta-autunite serve as structural references (**Figure S1**).

Four prominent peaks appear in the Fourier transforms (**Figure S2**, **right**) of the EXAFS spectra (**Figure S2**, **left**). The first two peaks can be assigned to O_{ax} (peak 1) and O_{eq} (peak 2). For both references peak 3 consist of multiple scattering events (MS) along the "yl" chain like the MS U-$O_{ax(1)}$-U-$O_{ax(2)}$. In the case of meta-autunite, the presence of P and the connected MS paths U-O_{eq}-P and U-O_{eq}-P- O_{eq} lead to an enhancement of peak 3 and the appearance of peak 4. The shell fit of these scattering signals is shown in **Figure S2** and their EXAFS structural parameters are listed in **Table S2**.

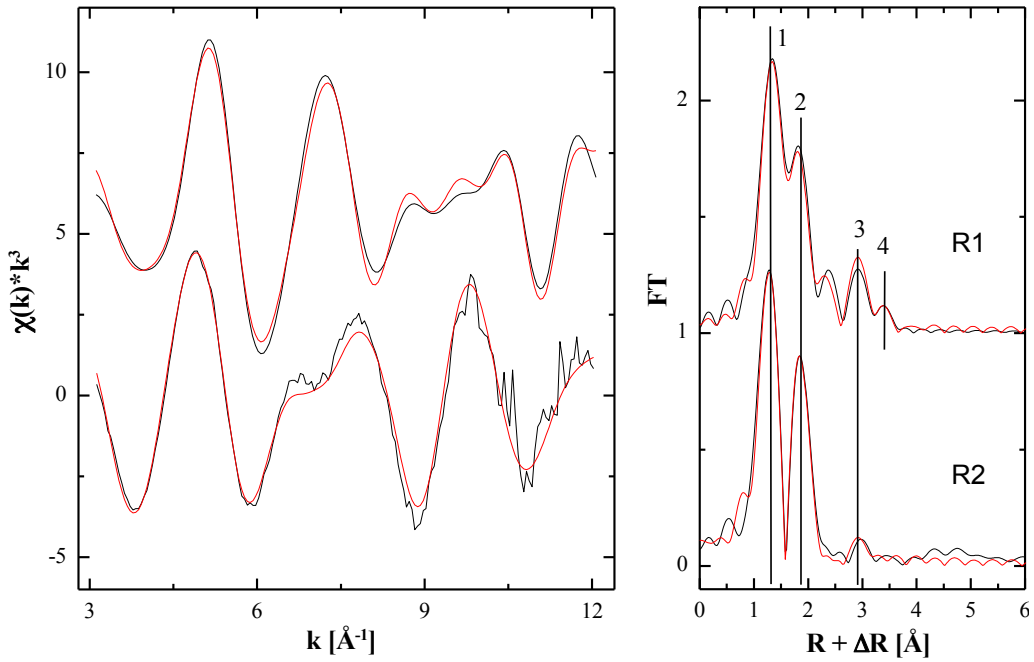

Figure S2. U L_{III}-edge EXAFS spectra of and meta-autunite (R1) and U(VI) hydrate (R2) (left, black) with shell fit (red) and corresponding Fourier transforms (right). The labeled FT peaks (1-4) are explained in the SI.

Table S2. Shell fit EXAFS structural parameters for the references meta-autunite and U(VI) hydrate.

Shell	*CN*	*R* / Å	σ^2 / Å^2	ΔE_0 / eV
meta-autunite (R1)				
O_{ax}	2*	1.7736(9) 1.79 [4]	0.00286(7)	0.7(2)
$U\text{-}O_{ax(1)}\text{-}U\text{-}O_{ax(2)}$	/2	/3.5472	/0.00572	/0.7
O_{eq}	4*	2.273(1) 2.33 [4]	0.00383(8)	/0.7
P	4*	3.605(3) 3.59 [4]	0.0029(2)	/0.7
$U\text{-}O_{eq}\text{-}P$	8*	3.734(4)	/0.0029(2)	/0.7
$U\text{-}O_{eq}\text{-}P\text{-}O_{eq}$	4*	/3.831	/0.0029(2)	/0.7
U(VI) hydrate (R2)				
O_{ax}	2*	1.757(2) 1.76 [5]	0.0018(2)	1.7(4)
$U\text{-}O_{ax(1)}\text{-}U\text{-}O_{ax(2)}$	/2	/3.514	/0.0036	/1.7
O_{eq}	4.6(3)	2.406(4) 2.40 [5]	0.0061(6)	/1.7

* - fixed parameter, /- linked parameter, *CN* – coordination number, *R* – radial distance, σ^2 – Debye-Waller factor, ΔE_0 – shift in energy threshold. The standard deviation of the fitted parameters is given in parentheses. Amplitude reduction factor $S_0^2 = 0.9$.

The EXAFS structural parameter are in good agreement with the values supplied by the literature (**Table S2**).

All sugar phosphate and DNA samples show the same four peaks (**Figure S3** and **Figure S5**) with different amplitudes for peak 2, 3 and 4 and different radial distances (*R*) in the case of peak 2, while only for peak 3 and peak 4 *R* does not change. These observations are in accordance with the exchange of coordinated water molecules by phosphate groups, hence with the fractional change of the scattering contributions of the selected references. Thus, for the determination of the *CN* of coordinated water molecules (CN_{water}) and phosphate groups ($CN_{phosphate}$) a linear mixing model, like ITFA, can be applied.

U(VI) with glucose-1-phosphate (G1P).

As the first step the PCA is performed. The *IND* function reaches a minimum at $n = 2$, hence all spectra can be sufficiently reproduced by two spectral components (**Figure S3**), even by inclusion of the two references. Thus, all spectra of the system U(VI)-G1P are linear combinations of the two selected references. In the last step and by keeping $CN_{water} = 5$ and $CN_{phosphate} = 4$ during the iteration, the ITT yields CN_{water} and $CN_{phosphate}$ for all samples (**Figure S4**). At pH = 2 U(VI) is already coordinated by one phosphate group, while at pH = 5 two phosphate groups, hence two G1P molecules, form a 1:2 U(VI):G1P complex. The small average relative error of 0.15 atoms in determination of the *CN* underpins the reliability of our proposed strategy for determination of $CN_{phosphate}$ in these chemical systems.

Table S3. Real error (*RE*) and indicator function (*IND*) in dependence of the number of spectral components (*n*) used for the reproduction of the U(VI)-G1P spectral mixtures.

Number of component (*n*)	*RE*	*IND*·10^4
1	0.102	15.9
2	0.069	14.1
3	0.066	18.4
4	0.064	25.4
5	0.061	38.3
6	0.059	65.4
7	0.056	140.5
8	0.054	536.7
9	-	-

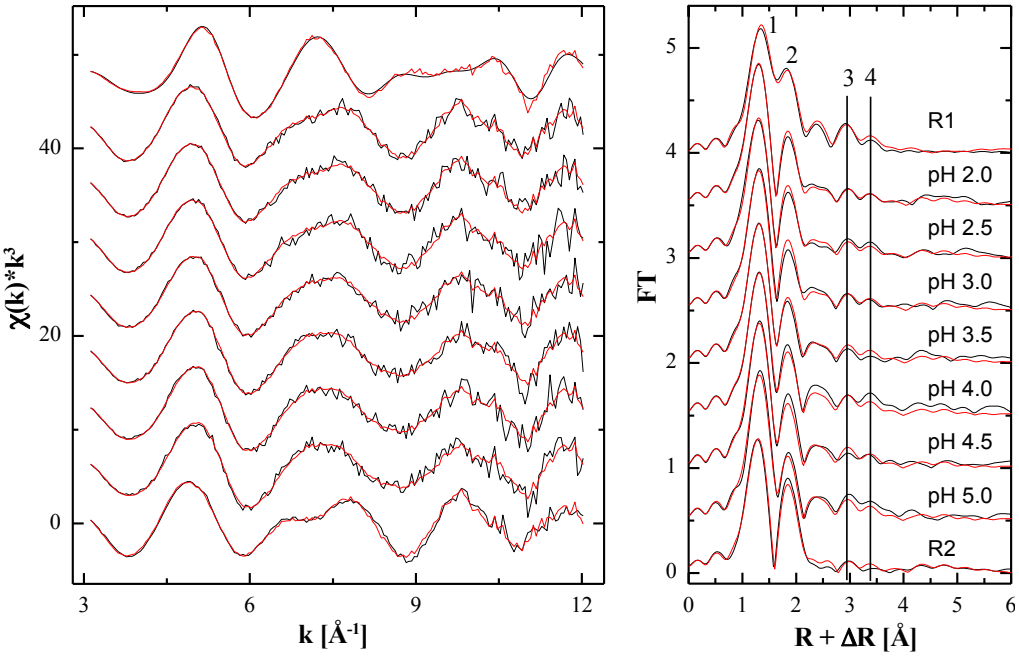

Figure S3. U L_{III}-edge EXAFS spectra of meta-autunite (R1), U(VI) hydrate (R2) and of the samples with G1P (**Table S1**) (left, black). Reproduction of the spectra by using two components (red). Corresponding Fourier transforms (right). The labeled FT peaks (1-4) are explained in the SI.

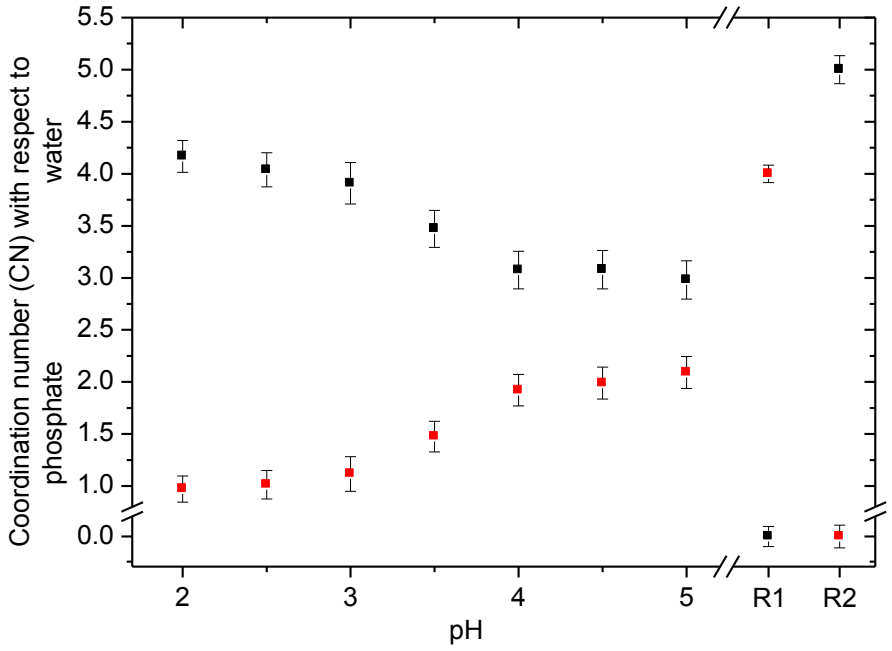

Figure S4. ITT determined *CN* of coordinated water molecules (black) and phosphate groups (red) in the case of the U(VI)-G1P system. R1 and R2 refer to the references meta-autunite and U(VI) hydrate, respectively. For each determined *CN* the estimated 95% confidence intervals are given.

U(VI) with DNA, fructose-6-phosphate (F6P) and fructose-1,6-diphosphate (F(1,6)P).

We used the same principle for determination of $CN_{phosphate}$ as applied in the case of U(VI) with G1P. Again, *IND* shows a minimum at two components (**Table S4**), hence the spectral mixtures can be sufficiently reproduced by using two components (**Figure S5**). The ITT determined CN_{water} and $CN_{phosphate}$ are listed in **Table S5**. The average relative error in determination of the *CN* of 0.1 atom is by a factor of 1.4 less than in the case of the U(VI)-G1P system. This observation can be explained with the determined root mean square error (*RE*) at $n = 2$, which can serve as a measure of the statistical error in the EXAFS spectra. The measured $RE_{n=2} = 0.049$ (**Table S4**) is by the same factor of 1.4 less than $RE_{n=2} = 0.069$ determined for the U(VI)-G1P system (**Table S3**), hence reflecting the better quality of the EXAFS spectra in the case of the samples with DNA, F6P and F(1,6)P which leads to the smaller error in *CN*.

The maximum $CN_{phosphate}$ equals two for samples M5 and M8 (**Table S1**, **Table S5**), hence maximum two sugar phosphate molecules coordinate U(VI) as in the case of U(VI) with G1P (**Figure S4**). We assume that the formation of complexes with a stoichiometry higher than 1:2 is sterically hindered due to the large size of the sugar phosphate molecules, since independently to the different chemical setup in sample preparation (**Table S1**) no 1:3 complexes were observed.

For U(VI) with DNA a maximum $CN_{phosphate} = 1.4\text{-}1.5$ is observed (M3 and M4, **Table S4**), hence values which point to the presence of 1:1 and 1:2 U(VI):DNA complexes where in the latter case the two phosphate groups might stem from the same DNA molecule.

Table S4. Real error (*RE*) and indicator function (*IND*) in dependence of the number of spectral components (*n*) used for the reproduction of the spectral mixtures of U(VI) with DNA, F6P and F(1,6)P.

Number of component (*n*)	*RE*	$IND \cdot 10^4$
1	0.085	8.5
2	0.049	6.0
3	0.045	7.0
4	0.040	8.2
5	0.034	9.5
6	0.030	12.1
7	0.026	16.4
8	0.023	25.9
9	0.020	50.8
10	0.017	167.8
11	-	

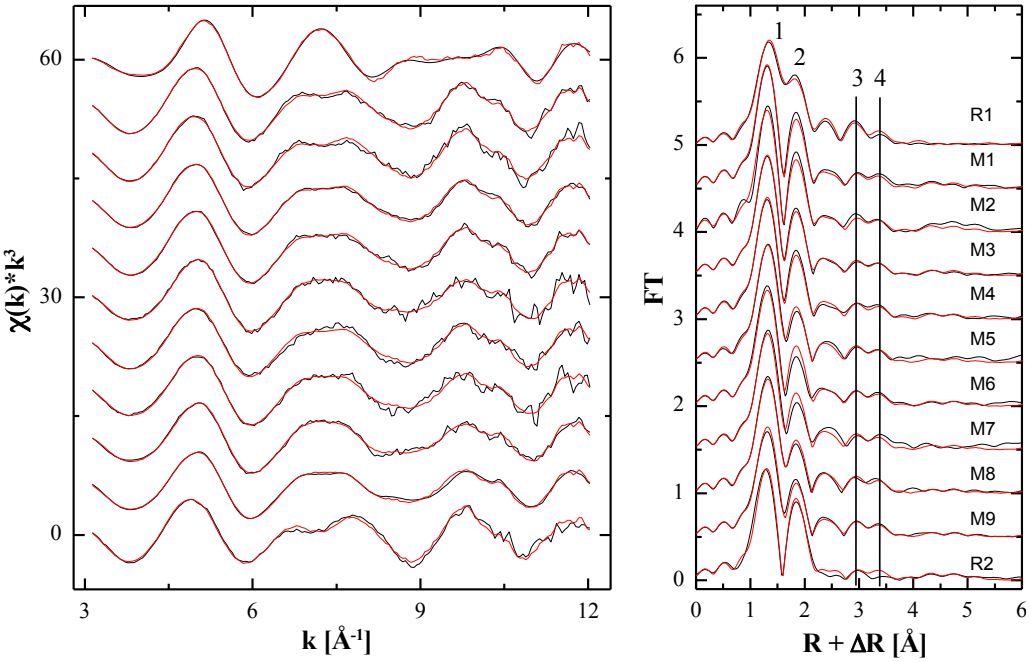

Figure S5. U L_{III}-edge EXAFS spectra of meta-autunite (R1), U(VI) hydrate (R2) and of the samples with DNA, F6P and F(1,6)P (M1-M9, **Table S1**) (left, black). Reproduction of the spectra by using two components (red). Corresponding Fourier transforms (right). The labeled FT peaks (1-4) are explained in the SI.

Table S5. ITT determined *CN* of coordinated water molecules (CN_{water}) and phosphate groups ($CN_{phosphate}$) in the case of the U(VI) with DNA, F6P and F(1,6)P. R1 and R2 refer to the references U(VI) hydrate and meta-autunite, respectively. For each determined *CN* the estimated 95% confidence intervals are given in parenthesis. Sample ID according **Table S1**.

Sample ID	CN_{water}	$CN_{phosphate}$
R1	0.00(9)	4.00(7)
M1	4.2(1)	1.20(8)
M2	4.4(1)	0.9(1)
M3	3.74(7)	1.43(6)
M4	3.73(9)	1.49(8)
M5	2.9(2)	2.1(1)
M6	3.5(1)	1.5(1)
M7	3.1(2)	1.8(1)
M8	2.6(1)	2.20(8)
M9	2.91(6)	1.73(5)
R2	5.0(1)	0.0(1)

Molecular dynamics simulation. MD simulations and data analyses were performed using AMBER 14 program package [24] with ff99SB force field applied on the protein. For UO_2^{2+} ions,[25] additional parameters were employed. The starting structure of Dickerson-Drew dodecamer was taken from a literature.[26] Na^+ ions were added to make the system electrostatically neutral. TIP3P waters were then added with minimum water layer thickness of 12 Å. 500 steps of steepest decent and 500 steps of conjugate gradient with 500 kcal mol^{-1} $Å^{-1}$ harmonic restraint on the DNA was initially conducted after which 1000 steps of steepest decent and 1500 steps of conjugate gradient were performed without constraints. 40 ps of heating of the system from 0 to 300 K with 10 kcal mol^{-1} $Å^{-1}$ harmonic restraint on the protein, after which another 1 ns preconditioning run was performed at 300 K without restraint on the solutes. Finally, 100 ns (for Structure A, without crosslink) or 150 ns MD (for Structure B, with crosslink) run was performed in a periodic boundary condition in NPT ensemble. Simulations were terminated and restarted at every 5 ns. The SHAKE algorithm, a 2 fs time integration step, 12 Å cutoff for non-bonded interactions, and the particle mesh Ewald (PME) method were used. MD trajectory was recorded at each 50 ps.

FMO calculations. The fragment molecular orbital (FMO) calculations were performed at the second-order Møller–Plesset perturbation (FMO-MP2) level [27-29] available in the ABINIT-MP program,[30] where a partial renormalization (PR-MP2) [31] was imposed to reduce overestimations in interaction energies. Several in-house Intel Xeon servers and the Fujitsu FX-100 system (Nagoya University) were employed for actual computations. The fragmentation for DNA was made in a standard segmentation manner (base, sugar, and phosphorous-acid units), and that the water molecules as well as Na+ counter ion were treated as single fragments. The basis sets for C, N, O, Na and P atoms was of valence double zeta plus polarization type of the model core potential (MCP) scheme.[32-33] Note that the use of MCP basis sets could reduce the basis set superposition error in evaluating interaction energies.[34] For U atom with large relativistic effect, a special MCP basis set (Miyoshi, unpublished) was used, where the 1s-5p electrons were replaced by the potentials and the valence electrons of 7s, 6d and 5f were described at the double zeta level. The standard 6-31G* [35] basis was adopted for H atoms. All the FMO calculations were performed with ABINIT-MP [30]: Nakano's local version with extended integral ability for the f-shell was used for the DNA plus uranyl system.

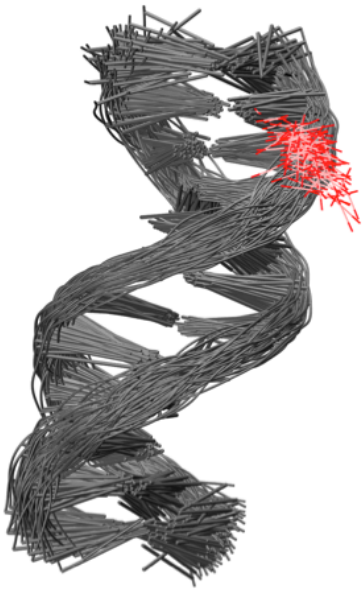

Figure S6. Superposition of 100 MD snapshots (each 1 ns for 100 ns) for simulation A in which no interstrand crosslink was observed.

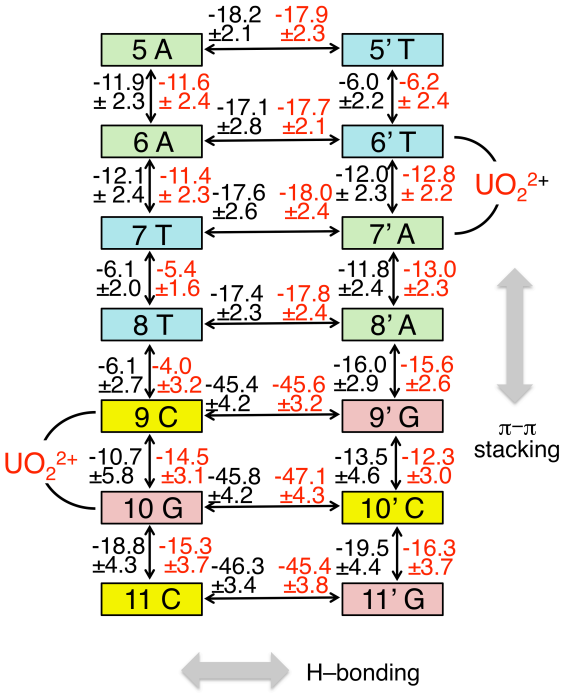

Figure S7. Average inter–fragment interaction energy (IFIE) amongst the nucleobases within DD dodecamer with (red) and without (black) UO_2^{2+} obtained by fragment molecular orbital calculations and their standard deviation (unit in kcal/mol). Two UO_2^{2+} depicted in the figure are identical UO_2^{2+} which is crosslinking the two strands across the minor groove.

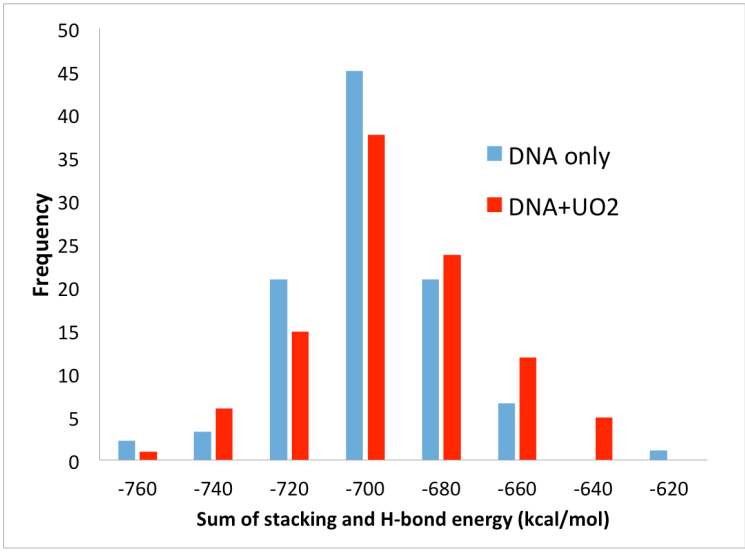

Figure S8. Histogram of the distribution of the sum of stacking energy and H-bond energy within Dickerson-Drew dodecamer with and without UO_2^{2+}.

References.

1. Reich, T.; Bernhard, G.; Geipel, G.; Funke, H.; Hennig, C.; Rossberg, A.; Matz, W.; Schell, N.; Nitsche, H. The Rossendorf Beam Line ROBL - a dedicated experimental station for XAFS measurements of actinides and other radionuclides. *Radiochim. Acta* **2000,** *88* (9-11), 633-637.
2. George, G. N.; Pickering, I. J. *EXAFSPAK: A Suite of Computer Programs for Analysis of X-ray Absorption Spectra*, Stanford Synchrotron Radiation Laboratory, Stanford, CA. USA., 1995.
3. Ankudinov, A. L.; Ravel, B.; Rehr, J. J.; Conradson, S. D. Real-space multiple-scattering calculation and interpretation of x-ray-absorption near-edge structure. *Physical Review B* **1998,** *58* (12), 7565-7576.
4. Makarov, E. S.; I., I. V. The crystal structure of meta-autunite, $Ca(UO_2)_2(PO_4)_2*6H_2O$ *Doklady Akademii Nauk SSSR* **1960,** *132*, 3.
5. Lucks, C.; Rossberg, A.; Tsushima, S.; Foerstendorf, H.; Scheinost, A. C.; Bernhard, G. Aqueous Uranium(VI) Complexes with Acetic and Succinic Acid: Speciation and Structure Revisited. *Inorganic Chemistry* **2012,** *51* (22), 12288-12300.
6. Rossberg, A.; Reich, T.; Bernhard, G. Complexation of uranium(VI) with protocatechuic acid - application of iterative transformation factor analysis to EXAFS spectroscopy. *Analytical and Bioanalytical Chemistry* **2003,** *376* (5), 631-638.
7. Breynaert, E.; Scheinost, A. C.; Dom, D.; Rossberg, A.; Vancluysen, J.; Gobechiya, E.; Kirschhock, C. E. A.; Maes, A. Reduction of Se(IV) in Boom Clay: XAS Solid Phase Speciation. *Environmental Science & Technology* **2010,** *44* (17), 6649-6655.
8. Froehlich, D. R.; Kremleva, A.; Rossberg, A.; Skerencak-Frech, A.; Koke, C.; Kruger, S.; Rosch, N.; Panak, P. J. Combined EXAFS Spectroscopic and Quantum Chemical Study on the Complex Formation of Am(III) with Formate. *Inorganic Chemistry* **2017,** *56* (12), 6820-6829.
9. Froehlich, D. R.; Skerencak-Frech, A.; Bauer, N.; Rossberg, A.; Panak, P. J. The pH dependence of Am(III) complexation with acetate: an EXAFS study. *Journal of Synchrotron Radiation* **2015,** *22*, 99-104.
10. Froehlich, D. R.; Skerencak-Frech, A.; Kaplan, U.; Koke, C.; Rossberg, A.; Panak, P. J. An EXAFS spectroscopic study of Am(III) complexation with lactate. *Journal of Synchrotron Radiation* **2015,** *22*, 1469-1474.

11. Ikeda, A.; Hennig, C.; Rossberg, A.; Tsushima, S.; Scheinost, A. C.; Bernhard, G. Structural determination of individual chemical species in a mixed system by iterative transformation factor analysis-based X-ray absorption spectroscopy combined with UV-visible absorption and quantum chemical calculation. *Analytical Chemistry* **2008,** *80* (4), 1102-1110.
12. Kirsch, R.; Fellhauer, D.; Altmaier, M.; Neck, V.; Rossberg, A.; Fanghanel, T.; Charlet, L.; Scheinost, A. C. Oxidation State and Local Structure of Plutonium Reacted with Magnetite, Mackinawite, and Chukanovite. *Environmental Science & Technology* **2011,** *45* (17), 7267-7274.
13. Pidchenko, I.; Kvashnina, K. O.; Yokosawa, T.; Finck, N.; Bahl, S.; Schild, D.; Polly, R.; Bohnert, E.; Rossberg, A.; Gottlicher, J.; Dardenne, K.; Rothe, J.; Schafer, T.; Geckeis, H.; Vitova, T. Uranium Redox Transformations after U(VI) Coprecipitation with Magnetite Nanoparticles. *Environmental Science & Technology* **2017,** *51* (4), 2217-2225.
14. Rossberg, A.; Ulrich, K. U.; Weiss, S.; Tsushima, S.; Hiemstra, T.; Scheinost, A. C. Identification of Uranyl Surface Complexes an Ferrihydrite: Advanced EXAFS Data Analysis and CD-MUSIC Modeling. *Environmental Science & Technology* **2009,** *43* (5), 1400-1406.
15. Scheinost, A. C.; Rossberg, A.; Vantelon, D.; Xifra, I.; Kretzschmar, R.; Leuz, A. K.; Funke, H.; Johnson, C. A. Quantitative antimony speciation in shooting-range soils by EXAFS spectroscopy. *Geochimica Et Cosmochimica Acta* **2006,** *70* (13), 3299-3312.
16. Ulrich, K. U.; Rossberg, A.; Foerstendorf, H.; Zanker, H.; Scheinost, A. C. Molecular characterization of uranium(VI) sorption complexes on iron(III)-rich acid mine water colloids. *Geochimica Et Cosmochimica Acta* **2006,** *70* (22), 5469-5487.
17. Malinowski, E. R. *Factor Analysis in Chemistry*. 2 ed.; John Wiley & Sons: New York, 1991.
18. Malinowski, E. R. Determination of the number of factors and the experimental error in a data matrix. *Analytical Chemistry* **1977,** *49* (4), 612-617.
19. Kaiser, H. F. The VARIMAX Criterion for Analytic Rotation in Factor Analysis. *Psychometrika* **1958,** *23* (3), 187-200.
20. Brayden, T. H.; Poropatic, P. A.; Watanabe, J. L. Iterative Target Testing for Calculation of Missing Data Points. *Analytical Chemistry* **1988,** *60* (11), 1154-1158.
21. Roscoe, B. A.; Hopke, P. K. Error-estimates for factor loadings and scores obtained with target transformation factor-analysis. *Analytica Chimica Acta* **1981,** *132* (DEC), 89-97.
22. Roscoe, B. A.; Hopke, P. K. Error-estimates for factor loadings and scores obtained by target transformation factor-analysis – A clarification. *Analytica Chimica Acta* **1982,** *135* (2), 379-380.
23. Koban, A.; Geipel, G.; Rossberg, A.; Bernhard, G. Uranium(VI) complexes with sugar phosphates in aqueous solution. *Radiochim. Acta* **2004,** *92* (12), 903-908.

24. Case D.A., Babin V., Berryman J.T., Betz R.M., Cai Q., Cerutti D.S., Cheatham T.E., III, Darden T.A., Duke R.E., Gohlke H., Goetz A.W., Gusarov S., Homeyer N., Janowski P., Kaus J., Kolossváry I., Kovalenko A., Lee T.S., LeGrand S., Luchko T., Luo R., Madej B., Merz K.M., Paesani F., Roe D.R., Roitberg A., Sagui C., Salomon-Ferrer R., Seabra G., Simmerling C.L., Smith W., Swails J., Walker R.C., Wang J., Wolf R.M., Wu X., Kollman P.A. Amber 14; University of California: San Francisco, CA, 2014.
25. Pomogaev, V., Tiwari, S.P., Rai, N., Goff, G.S., Runde, W., Schneider, W.F., Maginn, E.J. Development and application of effective pairwise potentials for UO_2^{n+}, NpO_2^{n+}, PuO_2^{n+}, and AmO_2^{n+} (n = 1, 2) ions with water. *Phys. Chem. Chem. Phys.* **201**3, 15, 15954–15963.
26. Lercher, L., McDonough, M.A., El-Sagheer, A.H., Thalhammer, A., Kriaucinois, S., Brown, T., Schofield, C.J. Structural insights into how 5-hydroxymethylation influences transcription factor binding. *Chem. Comm.* **2014,** 50, 1794–1796.
27. Mochizuki, Y., Nakano, T., Koikegami, S., Tanimori, S., Abe, Y., Nagashima, U., Kitaura, K. A parallelized integral-direct second-order Møller–Plesset perturbation theory method with a fragment molecular orbital scheme. *Theor. Chem. Acc.*, 2004, 112, 442-452.

28. Mochizuki, Y., Koikegami, S., Nakano, T., Amari, S., Kitaura, K. Large scale MP2 calculations with fragment molecular orbital scheme *Chem. Phys. Lett.*, 2004, 396, 473-479.
29. Mochizuki, Y., Yamashita, K., Murase, T., Nakano, T., Fukuzawa, K., Takematsu, K., Watanabe, H., Tanaka, S. Large scale FMO-MP2 calculations on a massively parallel-vector computer *Chem. Phys. Lett.*, 2008, 457 , 396-403.
30. Tanaka, S., Mochizuki, Y., Komeiji, Y., Okiyama, Y., Fukuzawa, K. Electron-correlated fragment-molecular-orbital calculations for biomolecular and nano systems *Phys. Chem. Chem. Phys.*, **2014**, 16, 10310-10344.
31. Dykstra, C. E. , Davidson, E. R. Enhanced second-order treatment of electron pair correlation. *Intern. J. Quant. Chem.*, 2000, 78, 226-236.
32. Ishikawa, T., Mochizuki, Y., Nakano, T., Amari, S., Mori, H., Honda, H. , Fujita, T., Tokiwa, H., Tanaka, S., Komeiji,Y., Fukuzawa, K., Tanaka, K., Miyoshi, E. Fragment molecular orbital calculations on large scale systems containing heavy metal atom *Chem. Phys. Lett.*, 2006, 427, 159-165.
33. Miyoshi, E., Mori, H., Hirayama, R., Osanai, Y., Noro, T., Honda, H., Klobukowski, M. Compact and efficient basis sets of *s*- and *p*-block elements for model core potential method *J. Chem. Phys.*, 2005, 122, 074104.
34. Yamada, H., Mochizuki, Y., Fukuzawa, K., Okiyama, Y., Komeiji, Y. Fragment molecular orbital (FMO) calculations on DNA by a scaled third-order Møller-Plesset perturbation (MP2.5) scheme *Comp. Theor. Chem.* 2017, 1101, 46-54.
35. Hariharan, P.C. , Pople, J.A. The influence of polarization functions on molecular orbital hydrogenation energies *Theor. Chimica Acta* 1973, 28, 213-222.